Density Functional Characterization of Methane Metathesis in *ansa*-[Bis(η^5-2-indenyl)methane]ML Complexes [M = Sc, Y, Lu; L = CH_3, $CH_2C(CH_3)_3$]

John L. Lewin, Nathaniel L. Woodrum, and Christopher J. Cramer*

Department of Chemistry and Supercomputer Institute, University of Minnesota, 207 Pleasant Street SE, Minneapolis, Minnesota 55455-0431

Received July 12, 2006

The uni- and bimolecular C−H bond metathesis reactions of *ansa*-[bis(η^5-2-indenyl)methane]ML (M = Sc, Y, Lu; L = CH_3, $CH_2C(CH_3)_3$) with four *ansa*-indenyl ligands having various degrees of aromatic ring methylation were modeled with the MPW1K density functional and a relativistic effective core potential basis set. Analysis of theoretical trends as a function of metal and ligand indicates that, in contrast to the situation with analogous $(Cp^*)_2$ sandwich complexes, unimolecular metathesis reactions proceeding through tuck-in intermediates have significantly higher enthalpies of activation compared to alternative bimolecular pathways, so that the latter dominate metathesis reactivity in every case under typical experimental conditions; taking account of quantum mechanical tunneling through the reaction coordinate does not change this situation. Narrow bite angles enforced by the *ansa* methylene bridge on the bis(indenyl) ligands cause the steric differences between methyl and neopentyl ligands to have reduced influence on either structural parameters or enthalpic barriers compared to analogous $(Cp^*)_2$ sandwich complexes. The degree of methylation of the bis(indenyl) ligand was found to play no significant role in complex structure and reactivity.

Introduction

The use of formally d^0 metallocenes as catalytic species is well established in olefin polymerization and is increasingly important in selective alicyclic and aliphatic C−H bond activation in organic synthesis.[1−3] Among the strongest organometallic C−H bond activators are the group III metallocenes incorporating scandium, yttrium, and lutetium metal centers.[2,3] We[4] and others[5] have been interested in the theoretical modeling of these species. Ongoing advances in computational technology[6] have made large metallocene complexes, such as those including the pentamethylcyclopentadienide $(Cp^*)^-$ ligand, increasingly amenable to full quantum mechanical treatment (as compared to, say, modeling via hybrid quantum mechanical/molecular mechanical techniques or through use of a smaller ligand model such as unmethylated Cp^-). Indeed, metallocenes as large as bis-indenyl sandwich complexes are now well within the realm of theoretical study. Of these, *ansa* bis-indenyl complexes, joined by various bridging groups at the 1 or 2 position of the indenyl moiety and potentially exhibiting chirality, depending on ring or bridge substitutions, are of special interest due to their enhanced activity and possible use for stereo- and enantioselective catalytic transformations.[2,3,7−16]

(1) (a) Togni, A., Halterman, R. L., Eds. *Metallocenes: Synthesis, Reactivity, Applications*; Wiley-VCH: Weinheim, 1998; Vols. 1 and 2. (b) Long, N. J. *Metallocenes: An Introduction to Sandwich Complexes*; Blackwell: Malden, MA, 1998; Chapters 1, 5, 6.

(2) (a) Watson, P. L.; Parshall, G. W. *Acc. Chem. Res.* **1985**, *18*, 51. (b) Davies, J. A.; Watson, P. L.; Liebman, J. F.; Greenberg, A. *Selective Hydrocarbon Activation: Principles and Progress*; VCH Publishers, Inc.: New York, 1990. (c) Shilov, A. E.; Shul'pin, G. B. *Chem. Rev.* **1997**, *97*, 2879. (d) Casey, C. P.; Klein, J. F.; Fagan, M. A. *J. Am. Chem. Soc.* **2000**, *122*, 4320. (e) Crabtree, R. H. *J. Chem. Soc., Dalton Trans.* **2001**, 2437. (f) Casey, C. P.; Tunge, J. A.; Lee, T. Y.; Carpenetti, D. W. *Organometallics* **2002**, *21*, 389. (g) Sadow, A.; Tilley, T. D. *Angew. Chem., Int. Ed.* **2003**, *42*, 803. (h) Sadow, A. D.; Tilley, T. D. *J. Am. Chem. Soc.* **2003**, *125*, 7971. (i) Hong, S.; Marks, T. J. *Acc. Chem. Res.* **2004**, *37*, 673.

(3) (a) Watson, P. L. *J. Chem. Soc., Chem. Commun.* **1983**, 276. (b) Watson, P. L. *J. Am. Chem. Soc.* **1983**, *105*, 6491. (c) Watson, P. L. In *Selective Hydrocarbon Activation: Principles and Progress*; Davies, J. A., Watson, P. L., Greenberg, A., Liebman, J. F., Eds.; VCH: New York, 1990; p 79. (d) Evans, W.; Foster, S. E. *J. Organomet. Chem.* **1992**, *433*, 79. (e) Haar, C. M.; Stern, C. L.; Marks, T. J. *Organometallics* **1996**, *15*, 1765. (f) Chirik, P. J.; Bercaw, J. E. In *Metallocenes: Synthesis, Reactivity, Applications*; Togni, A., Halterman, R. L., Eds.; Wiley-VCH: Weinheim, 1998; Vol. 1, Chapter 3. (g) Schumann, H.; Keitsch, M. R.; Winterfeld, J.; Muhle, S.; Molander, G. A. *J. Organomet. Chem.* **1998**, *559*, 181. (h) Schumann, H.; Rosenthal, E. C. E.; Demtschuk, J. *Organometallics* **1998**, *17*, 5324.

(4) (a) Sherer, E. C.; Cramer, C. J. *Organometallics* **2003**, *22*, 1682. (b) Woodrum, N. L.; Cramer, C. J. *Organometallics* **2006**, *25*, 68. (c) Woodrum, N. M.S. Thesis, University of Minnesota−Twin Cities, 2005.

(5) (a) Folga, E.; Ziegler, T.; Fan, L. *New J. Chem.* **1991**, *15*, 741. (b) Folga, E.; Ziegler, T. *Can. J. Chem.* **1992**, *70*, 333. (c) Rappe, A. K.; Upton, T. H. *J. Am. Chem. Soc.* **1992**, *114*, 7507. (d) Ziegler, T.; Folga, E.; Berces, A. *J. Am. Chem. Soc.* **1993**, *115*, 636. (e) Ziegler, T.; Folga, E. *J. Organomet. Chem.* **1994**, *478*, 57. (f) Adamo, C.; Barone, V. *J. Comput. Chem.* **2000**, *21*, 1153. (g) Maron, L.; Eisenstein, O. *J. Phys. Chem.* **2000**, *104*, 7140. (h) Niu, S. Q.; Hall, M. B. *Chem. Rev.* **2000**, *100*, 353. (i) Ustynyuk, Y. A.; Ustynyuk, L. Y.; Laikov, D. N.; Lunin, V. V. *J. Organomet. Chem.* **2000**, *597*, 182. (j) Maron, L.; Eisenstein, O. *J. Am. Chem. Soc.* **2001**, *123*, 1036. (k) Maron, L.; Eisenstein, O.; Alary, F.; Poteau, R. *J. Phys. Chem.* **2002**, *106*, 1797. (l) Maron, L.; Perrin, L.; Eisenstein, O. *J. Chem. Soc., Dalton Trans.* **2002**, 534. (m) Perrin, L.; Maron, L.; Eisenstein, O. *Inorg. Chem.* **2002**, *41*, 4355. (n) Maron, L.; Perrin, L.; Eisenstein, O. *Dalton Trans.* **2003**, *22*, 4313. (o) Perrin, L.; Maron, L.; Eisenstein, O. *New J. Chem.* **2004**, *28*, 1255. (p) Rotzinger, F. P. *Chem. Rev.* **2005**, *105*, 2003. (q) Barros, N.; Eisenstein, O.; Maron, L. *Dalton Trans.* **2006**, 3052. (r) Baisch, U.; Pagano, S.; Zeuner, M.; Barros, N.; Maron, L.; Schnick, W. *Chem. Eur. J.* **2006**, *12*, 4785. (s) Roger, M.; Barros, N.; Arliguie, T.; Thuery, P.; Maron, L.; Ephritikhine, M. *J. Am. Chem. Soc.* **2006**, *128*, 8790. (t) De, Almeida, K. J.; Cesar, A. *Organometallics* **2006**, *25*, 3407. (u) Raynaud, C.; Perrin, L.; Maron, L. *Organometallics* **2006**, *25*, 3143.

(6) Cramer, C. J. *Essentials of Computational Chemistry: Theories and Models*, 2nd ed.; Wiley: Chichester, 2004.

(7) Bradley, C. A.; Keresztes, I.; Lobkovsky, E.; Chirik, P. J. *Organometallics* **2006**, *25*, 2080.

(8) Green, J. C. *Chem. Soc. Rev.* **1998**, *27*, 263.

(9) Hitchcock, S. R.; Situ, J. J.; Covel, J. A.; Olmstead, M. M.; Nantz, M. H. *Organometallics* **1995**, *14*, 3732.

10.1021/om0606237 CCC: $33.50
Publication on Web 11/08/2006

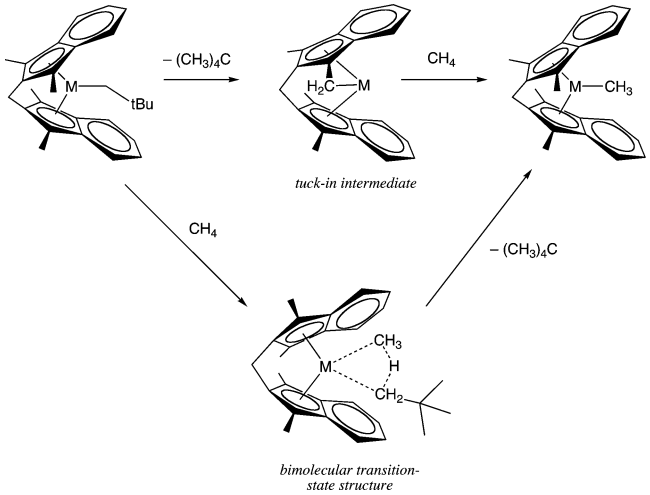

Figure 1. Uni- and bimolecular metathesis reactions available to a neopentyl *ansa*-metallocene.

In prior work,[4] we characterized the uni- and bimolecular metathesis reactions of $(Cp^*)_2ML$ for M = scandium, yttrium, and lutetium, and alkyl group L = methyl and neopentyl. We found that bimolecular reaction with methane was kinetically the most favorable process under typical reaction conditions, although with metals having a smaller radius (e.g., M = Sc) or more sterically demanding alkyl groups (e.g., L = neopentyl), unimolecular reactions proceeding through a tuck-in complex became increasingly competitive. We also established that quantum mechanical tunneling along either uni- or bimolecular H atom transfer coordinates increases the corresponding reaction rate constants by 2 to 3 orders of magnitude at typical reaction temperatures of 300−400 K.

In this article, we extend our prior studies to address analogous, larger complexes supported by the dianionic ligand derived from bis(2-indenyl)methane. We assess the effect of the methylene-bridged *ansa* ligand on metallocene geometries and activation enthalpies (again, for both uni- and bimolecular reactions, see Figure 1), and we quantify the degree to which quantum mechanical tunneling contributes to overall reaction rates. In addition, we examine the degree to which methylation of the indenyl ligands affects these various phenomena.

Computational Methods

All structures were fully optimized at the density functional level of theory[17] using the GAUSSIAN 03 (rev. C.01) suite of electronic structure programs.[18] In this work we employ the hybrid MPW1K functional,[19] which includes 42.8% Hartree−Fock (HF) exchange in Adamo and Barone's one-parameter modification[20] of the combined hybrid generalized gradient approximation exchange[21] and correlation[22] functionals of Perdew and Wang (*m*PW1PW). Since the amount of HF exchange in the MPW1K functional was optimized to best reproduce a set of experimental activation energies for hydrogen atom transfer reactions, MPW1K is a particularly appropriate functional for the study of C−H bond metathesis reactions. In addition, the MPW1K functional has also been demonstrated to do well in predicting a wide variety of other structural and thermochemical data.[6] With respect to basis sets, we employed the relativistic effective core potentials and valence basis sets of Stoll et al.[23] for Sc, Y, and Lu and the 6-31G(d,p) basis set[24] for H and C.

Stationary points on the potential energy surface (PES) were verified as minima or transition-state (TS) structures by analytic frequency calculations. The real frequencies, scaled by a factor of 0.9515,[25] were additionally employed to compute molecular partition functions and thermal contributions to the enthalpy using the standard rigid-rotor harmonic-oscillator approximation at 299 K.[6] Scaled imaginary frequencies in TS structures were used in the calculation of quantum mechanical transmission coefficients. Because structures incorporating methylated aromatic rings typically had one or more very small vibrational frequencies (e.g., below 20 cm^{-1}), we avoid for the most part discussion of molecular free energies, since absolute entropies predicted by the rigid-rotor harmonic-oscillator approximation tend to be unreliable in such instances.

Since the reaction coordinates for the C−H bond metatheses examined here involve substantial hydrogenic motion near the transition state, one expects[4] that the reaction rate will include a significant contribution from light-atom tunneling even at reaction temperatures of about 350 K. Within the context of transition-state theory, the observed rate constant k_{obs} may be written as[6,26]

$$k_{obs} = \kappa(T) k_{class} \tag{1}$$

where κ is the temperature-dependent quantum mechanical transmission coefficient and k_{class} is the rate constant that would be observed in the *absence* of quantum effects, i.e., the classical rate constant.

Experimentally, activation enthalpies and entropies are often derived from the Eyring relationship[6,26]

$$\ln\left(\frac{k_{obs}}{T}\right) = -\frac{\Delta H^{\ddagger}}{R}\left(\frac{1}{T}\right) + \frac{\Delta S^{\ddagger}}{R} + \ln\left(\frac{k_B}{h}\right) \tag{2}$$

where T is temperature in degrees kelvin, R is the universal gas

(10) Hoveyda, A. H.; Morken, J. P. In *Metallocenes: Synthesis, Reactivity, Applications*; Togni, A., Halterman, R. L., Eds.; Wiley-VCH: Weinheim, 1998; Vol. 2, Chapter 10.
(11) Prashar, S.; Antiñolo, A.; Otero, A. *Coord. Chem. Rev.* **2006**, *250*, 133.
(12) Resconi, L. *Polym. Prepr. (Am. Chem. Soc. Div. Polym. Chem.)* **2002**, *43*, 303.
(13) Schumann, H.; Erbstein, F.; Karasiak, D. F.; Fedushkin, I. L.; Demtschuk, J.; Girgsdies, F. *Z. Anorg. Allg. Chem.* **1999**, *625*, 781.
(14) Shaltout, R. M.; Corey, J. Y.; Rath, N. P. *J. Organomet. Chem.* **1995**, *503*, 205.
(15) Shapiro, P. J. *Coord. Chem. Rev.* **2002**, *231*, 67.
(16) Wang, B. *Coord. Chem. Rev.* **2006**, *250*, 242.
(17) Koch, W.; Holthausen, M. C. *A Chemist's Guide to Density Functional Theory*; Wiley-VCH: Weinheim, 2000.
(18) Frisch, M. J.; Trucks, G. W.; Schlegel, H. B.; Scuseria, G. E.; Robb, M. A.; Cheeseman, J. R.; Montgomery, Jr., J. A.; Vreven, T.; Kudin, K. N.; Burant, J. C.; Millam, J. M.; Iyengar, S. S.; Tomasi, J.; Barone, V.; Mennucci, B.; Cossi, M.; Scalmani, G.; Rega, N.; Petersson, G. A.; Nakatsuji, H.; Hada, M.; Ehara, M.; Toyota, K.; Fukuda, R.; Hasegawa, J.; Ishida, M.; Nakajima, T.; Honda, Y.; Kitao, O.; Nakai, H.; Klene, M.; Li, X.; Knox, J. E.; Hratchian, H. P.; Cross, J. B.; Bakken, V.; Adamo, C.; Jaramillo, J.; Gomperts, R.; Stratmann, R. E.; Yazyev, O.; Austin, A. J.; Cammi, R.; Pomelli, C.; Ochterski, J. W.; Ayala, P. Y.; Morokuma, K.; Voth, G. A.; Salvador, P.; Dannenberg, J. J.; Zakrzewski, V. G.; Dapprich, S.; Daniels, A. D.; Strain, M. C.; Farkas, O.; Malick, D. K.; Rabuck, A. D.; Raghavachari, K.; Foresman, J. B.; Ortiz, J. V.; Cui, Q.; Baboul, A. G.; Clifford, S.; Cioslowski, J.; Stefanov, B. B.; Liu, G.; Liashenko, A.; Piskorz, P.; Komaromi, I.; Martin, R. L.; Fox, D. J.; Keith, T.; Al-Laham, M. A.; Peng, C. Y.; Nanayakkara, A.; Challacombe, M.; Gill, P. M. W.; Johnson, B.; Chen, W.; Wong, M. W.; Gonzalez, C.; and Pople, J. A. *Gaussian 03 (Revision C.01)*; Gaussian, Inc.: Wallingford, CT, 2004.
(19) Lynch, B. J.; Fast, P. L.; Harris, M.; Truhlar, D. G. *J. Phys. Chem. A* **2000**, *104*, 4811.
(20) Adamo, C.; Barone, V. *J. Chem. Phys.* **1998**, *108*, 664.
(21) Perdew, J. P.; Wang, Y. *Phys. Rev. B* **1986**, *33*, 8800.
(22) Perdew, J. P. In *Electronic Structure of Solids '91*; Ziesche, P., Eschrig, H., Eds.; Akademie Verlag: Berlin, 1991; p 11.
(23) Stoll, H.; Metz, B.; Dolg, M. *J. Comput. Chem.* **2002**, *23*, 767.
(24) Hehre, W. J.; Radom, L.; Schleyer, P. v. R.; Pople, J. A. In *Ab Initio Molecular Orbital Theory*; Wiley: New York, 1986.
(25) Lynch, B. J.; Truhlar, D. G. *J. Phys. Chem. A* **2001**, *105*, 2936.
(26) Steinfeld, J. I.; Francisco, J. S.; Hase, W. L. *Chemical Kinetics and Dynamics*, 2nd ed.; Prentice Hall: New York, 1999.

constant, k_B is Boltzmann's constant, and h is Planck's constant. A plot of $\ln(k_{obs}/T)$ versus $1/T$ provides a best-fit line having a slope $-\Delta H^{\ddagger}/R$ and an intercept $\Delta S^{\ddagger}/R$. However, the determination of these thermodynamic activation parameters using eq 2 is only appropriate when the transmission coefficient κ is equal to 1, i.e., in the absence of tunneling contributions so that the observed rate constant corresponds to the *classical* rate constant.[4] When eq 2 is used with observed rate constants from reactions whose rates include substantial contributions from tunneling, the derived activation enthalpies and entropies tend to values considerably less positive and more negative, respectively, than those more properly determined from the statistical-mechanical partition functions of the relevant reactants and transition-state structures. In such instances, the comparison of "experimental" and computed thermodynamic activation parameters is not particularly meaningful, since the latter are indeed computed properly from the molecular partition functions and are not masked by tunneling contributions.

With the experimental data in hand, however, one can compute the classical rate constant k_{class} at a given temperature as k_{obs} divided by $\kappa(T)$ (cf. eq 1) provided one has some means of estimating κ. A subsequent plot of $\ln(k_{class}/T)$ versus $1/T$ then provides a best-fit line having a slope $-\Delta H^{\ddagger}/R$, where the new, classical $\Delta H^{\ddagger}$ may be compared directly to the value derived from computation of the relevant partition functions. Sherer and Cramer have previously demonstrated that this protocol resolves an otherwise large difference of 7.6 kcal mol^{-1} in the "experimental" and computed enthalpies of activation for methane metathesis involving $(Cp^*)_2LuCH_3$.[4a] In order to estimate κ, we employ the truncated parabola method of Skodje and Truhlar.[27] In this one-dimensional approximation, the transmission coefficient associated with quantum effects on the reaction coordinate is computed as

$$\kappa(T) = \frac{\beta\pi/\alpha}{\sin(\beta\pi/\alpha)} - \frac{\beta}{\alpha - \beta}\exp[(\beta - \alpha)(\Delta V^{\ddagger} - V)] \qquad \beta \leq \alpha \tag{3a}$$

$$\kappa(T) = \frac{\beta}{\beta - \alpha}\{\exp[(\beta - \alpha)(\Delta V^{\ddagger} - V)] - 1\} \qquad \alpha \leq \beta \tag{3b}$$

where

$$\alpha = \frac{2\pi}{h\{\mathrm{Im}(\nu^{\ddagger})\}}, \tag{4}$$

$$\beta = \frac{1}{k_B T}, \tag{5}$$

$\Delta V^{\ddagger}$ is the zero-point-including activation potential energy, V is the zero-point-including potential energy difference between reactants and products (zero in the case of a symmetric metathesis reaction, nonzero otherwise), and $\mathrm{Im}(\nu^{\ddagger})$ is the (scaled) magnitude of the imaginary vibration.

Results and Discussion

Nomenclature. We consider four distinct *ansa* ligands differing in the degree of methylation of the indenyl rings. In particular, we employ the dianionic ligands derived from bis(1,3-dimethyl-2-indenyl)methane, bis(1,3,4,7-tetramethyl-2-indenyl)methane, bis(1,3,4,5,6,7-hexamethyl-2-indenyl)methane, and bis(4,5,6,7-tetramethyl-2-indenyl)methane. We refer to metallocenes derived from these ligands as **1**, **2**, **3**, and **4**, respectively (Chart 1). Note that ligand **4** is unique inasmuch as the five-membered ring is *not* methylated, and metallocenes **4** thus cannot form tuck-in complexes from unimolecular methathesis.

(27) Skodje, R. T.; Truhlar, D. G. *J. Phys. Chem.* **1981**, *85*, 624.

Chart 1

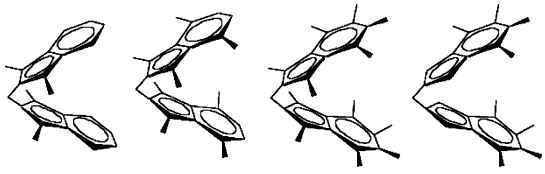

1 **2** **3** **4**

Table 1. *D* Parameter Values (Å) in *ansa*-Indenyl and Cp* Metallocenes at the MPW1K Level

	ligand system				
metal	$(Cp^*)_2$[a]	**1**	**2**	**3**	**4**
L = Me					
Sc	0.676	1.085	1.103	1.071	1.084
Y	0.754	1.320	1.313	1.312	1.324
Lu	0.697	1.235	1.227	1.223	1.239
L = Np					
Sc	0.784	1.124	1.124	1.114	1.122
Y	0.856	1.341	1.330	1.326	1.341
Lu	0.829	1.263	1.249	1.250	1.263

[a] Values computed from data in ref 4b, included for comparison.

Each metallocene **1**−**4** was further substituted by a methyl (Me) or neopentyl (Np) ligand L. In this work a particular species will be referred to as cardinal number-metal-alkyl fragment (or tuck-in), for example **1**-Sc-Me refers to [bis(1,3-dimethyl-2-indenyl)methane]scandium methide. Transition-state structures are indicated by the inclusion immediately after the cardinal of uni‡ or bi‡ for uni- and bimolecular metathesis transition states, respectively, e.g., **1**uni‡-Sc-Me for the unimolecular TS structure of **1**-Sc-Me.

***ansa*-Metallocene Structures**. Selected geometrical parameters for the equilibrium minimum-energy structures of **1**−**4** are shown in Table S1 of the Supporting Information; data for the analogous $(Cp^*)_2ML$ systems[4] are included for comparison. Optimized geometries of **3**-Sc-Me, chosen as a representative example, are shown in Figure 2.

We find that there is relatively little variation of geometry as a function of *ansa* ligand for a given metal and alkyl ligand. However, there is a consistent, small increase in the metal−alkyl carbon bond length proceeding from **1** to **2** to **3**. This is consistent with increased methylation in the progression, making the *ansa* ligand increasingly electron donating. Of course, the bite angle enforced by the bridging methylene reduces the ability of the aromatic rings to overlap with metal orbitals as efficiently as they do in the unconstrained $(Cp^*)_2ML$, and consistent with this analysis the metal−alkyl carbon bond lengths are the longest of all in the $(Cp^*)_2ML$ compounds. The difference is particularly large for L = Np, where steric interactions between the neopentyl ligand and the Cp* rings appear to develop, so that the bite angle of the two Cp* rings is reduced in $(Cp^*)_2MNp$ relative to $(Cp^*)_2MMe$, but the metal−Np bond length is lengthened as well so as not to sacrifice too much overlap of the aromatic rings with the metal d orbitals.

Trends as a function of metal are consistent for each *ansa* ligand set: shorter ligand−metal bond lengths and larger bite angles are observed for scandium compared to yttrium, consistent with a typical third-row to fourth-row progression. Relativistic effects and the lanthanide contraction come into play for lutetium compared to yttrium, and slightly shorter ligand−metal bond lengths and slightly larger bite angles are observed for the former compared to the latter.

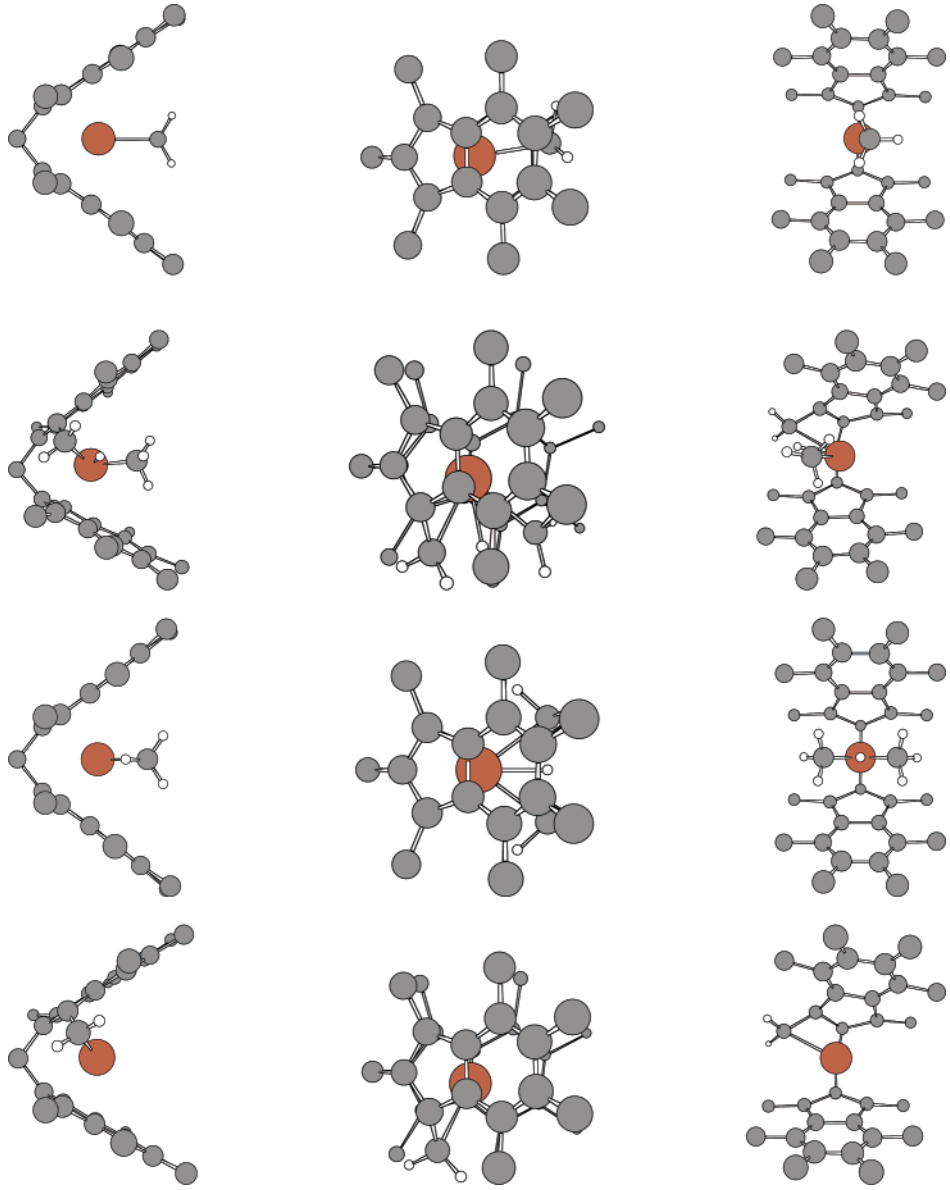

Figure 2. Optimized structures (MPW1K) shown in side-on (left and right) and top (center) views for (from top to bottom) **3**-Sc-Me, **3**uni‡-Sc-Me, **3**bi‡-Sc-Me, and **3**-Sc-tuck-in. Hydrogen atoms not attached to or being transferred from carbon atoms bonded to scandium have been removed for clarity.

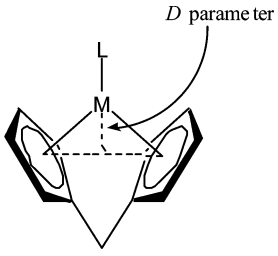

Figure 3. Definition of the *D* parameter (Å) in a generic *ansa* metallocene system. The position of the 5-membered ring centroid defines Ω.

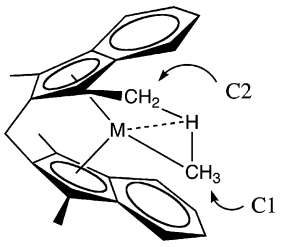

Figure 4. Coordinate definitions used for discussion of tuck-in TS structures.

The bridging methylene induces a reduction in the Ω−M−Ω angle from about 143° in the unconstrained metallocenes to about 120°, 112°, and 114° for the *ansa* Sc, Y, and Lu systems, respectively. The effect of the *ansa* bridge can also be quantified by the *D* parameter, defined as the perpendicular distance of the metal atom from the imaginary line connecting the centroids of the two five-membered rings, which may be computed from the trigonometric relationship between *r*MΩ and $^1/_2$-(∠ΩMΩ);[8,14,15] see Figure 3 and Table 1.

The difference between Cp* and the *ansa* indenyl ligand is most pronounced in the L = Me cases, where the average percent change in *D* ranges from 61% in scandium species, to 75% in yttrium, to 77% in lutetium. The change is smaller in the L = Np complexes, as the bulky neopentyl group forces a longer *r*MΩ distance and smaller ∠ΩMΩ in the $(Cp^*)_2$ system

Table 2. Relative Enthalpies (kcal mol^{-1}, 299 K) for Stationary Points on the Unimolecular Reaction Coordinates for *ansa* Ligands 1−3 and Quantum Mechanical Transmission Coefficients (unitless) for Their Rate-Determining Steps

ligand	metal	Me	uni‡	tuck-in	reverse‡	Me	κ_{299}
L = methyl							
$(Cp^*)_2$[a]	Sc	0.0	30.6	8.0	30.6	0.0	110
	Y	0.0	32.3	13.3	32.3	0.0	190
	Lu	0.0	32.8	14.1	32.8	0.0	120
1	Sc	0.0	34.1	19.9	34.1	0.0	56
	Y	0.0	34.5	16.6	34.5	0.0	150
	Lu	0.0	36.0	21.1	36.0	0.0	75
2	Sc	0.0	34.0	20.0	34.0	0.0	61
	Y	0.0	34.2	17.2	34.2	0.0	150
	Lu	0.0	35.6	21.4	35.6	0.0	76
3	Sc	0.0	34.0	19.4	34.0	0.0	59
	Y	0.0	35.0	17.1	35.0	0.0	180
	Lu	0.0	35.7	20.9	35.7	0.0	79

ligand	metal	Np	uni‡	tuck-in	reverse$^{\ddagger\text{HardReturn}}$(w/$CH_4$)	Me	κ_{299}
L = neopentyl							
$(Cp^*)_2$[a]	Sc	0.0	27.2	−7.8	14.8	−15.8	280
	Y	0.0	29.4	2.7	21.7	−10.6	1200
	Lu	0.0	29.8	1.8	20.5	−12.2	1000
1	Sc	0.0	31.6	11.9	26.2	−7.9	58
	Y	0.0	33.5	12.3	30.2	−4.3	260
	Lu	0.0	34.1	15.9	30.8	−5.2	97
2	Sc	0.0	31.5	11.9	25.9	−8.2	70
	Y	0.0	33.4	12.8	29.8	−4.4	240
	Lu	0.0	34.0	16.4	30.6	−5.1	100
3	Sc	0.0	31.8	11.9	26.6	−7.5	63
	Y	0.0	34.0	13.0	30.9	−4.1	300
	Lu	0.0	34.3	16.1	30.8	−4.9	110

[a] Values taken from ref 4b.

as noted above, but the difference is still substantial. The overriding structural constraints of the methylene bridge are manifest in the similar *D* values of the methyl- and neopentyl-alkylated *ansa* complexes, which contrasts with the situation in the free Cp* metallocenes, where variation of *D* as a function of the alkyl ligand is about 5 times larger. The *D* values and bite angles computed here are consistent with those from X-ray crystal structural data reported by Agarkov et al.[28] for isomeric *ansa*-[bis(η^5-1-indenyl)methane]MCl_2 compounds. With M = Ti, Zr, and Hf, these authors observed average bite angles of 122°, 117°, and 118°, respectively, and *D* values of 1.028, 1.149, and 1.126 Å, respectively; the slightly smaller *D* values in this case are consistent with the slightly smaller radii of the group IV metals. Data are also available for metallocenes carring bis-(indenyl)silane ligands,[29] but as there is a significant difference in the bond length to the bridging silicon compared to carbon atom, we do not make comparisons here.

Geometrical parameters for the uni- and bimolecular TS structures are compiled in Tables S2 and S3, respectively, of the Supporting Information. While the data are for the most part routine (and thus left to languish in the Supporting Information), a few features *are* noteworthy. Metal−alkyl bond distances show the same trends as a function of *ansa* ligand in the TS structures as are observed in the minima: more alkylation of the indenyl rings leads to increased bond lengths. In the unimolecular TS structures, the bond length from the metal to the ring methyl group does not show such variation, presumably because of the dominance of geometric constraints associated with *ansa* ligation of the metal itself. Focusing on the C−H bond lengths to the H atom in flight, the unimolecular reactions involving M = Lu exhibit late transition states (with the forming bond to C1 substantially shorter than the breaking bond to C2; see Figure 4), consistent with formation of the tuck-in complex for M = Lu being more endothermic than for either Sc or Y in each case of **1**−**3** (see below). The earliest transition states (short breaking bond to C2, long forming bond to C1) are associated with **1**uni‡-Y-Np and **3**uni‡-Y-Np, for which cases formation of the tuck-in complex is 3−4 kcal/mol less endothermic than for the Lu cases. Interestingly, when M = Sc, the unimolecular TS structures show little difference in forming and breaking C−H bond lengths, even though the endothermicity of formation of the tuck-in complex for M = Sc is slightly smaller than for M = Y. It is possible that this results from a much stronger interaction between the metal and the H atom in flight in the case of M = Sc; the average Sc−H bond length is about 1.86 Å compared to 1.97 Å for M = Lu and 2.03 Å for M = Y.

Compared to the unimolecular TS structures, the bimolecular TS structures tend to have much shorter making and breaking bond lengths between the H atom in flight and the incoming and outgoing alkyl groups, suggesting a significant reduction of strain in the geometry of the bimolecular TS structures. For L = Me, structures **1**bi‡−**4**bi‡ are symmetric for M = Sc and Lu. However, in the case of M = Y the two indenyl rings in the *ansa* ligand do not eclipse one another perfectly, so that the TS structure is asymmetric. This twisting of the ansa ligand is observed in several of the minimum-energy structures as well, although it is quite small. In other cases, any barrier associated with a conversion between formally enantiomeric *ansa* twists is sufficiently small that this motion is included in the H atom transfer reaction coordinate, but that is not the case for M = Y. However, relaxation of the *ansa* rings will obviously not be rate determining for the metathesis step when M = Y, so we have not examined this process in any detail. For L = Np, the TS structures are noticeably early in every case: differences in

(28) Agarkov, A. Y.; Izmer, V. V.; Riabov, A. N.; Kuz'mina, L. G.; Howard, J. A. K.; Beletskaya, I. P.; Voskoboynikov, A. Z. *J. Organomet. Chem.* **2001**, *619*, 280.

(29) (a) Giardello, M. A.; Conticello, V. P.; Brard, L.; Sabat, M.; Rheingold, A. L.; Stern, C. L.; Marks, T. J. *J. Am. Chem. Soc.* **1994**, *116*, 10212. (b) Herrmann, W. A.; Eppinger, J.; Spiegler, M.; Runte, O.; Anwander, R. *Organometallics* **1997**, *16*, 1813.

forming and breaking C−H bond lengths are as large as 0.1 Å. This observation is consistent with the strain release associated with the replacement of L = Np by L = Me, and an even larger effect was observed previously for the unconstrained case of $(Cp^*)_2MNp$,[4] where the steric clash between the Np ligand and the Cp* rings is increased relative to the *ansa* ligands examined here.

Tables S2 and S3 also include the imaginary frequencies characterizing the TS structures. The magnitudes of the imaginary frequencies associated with the unimolecular TS structures range from 1350 to 1450 cm^{-1}, and in every case these frequencies are larger in magnitude than are those associated with the corresponding bimolecular transition states. That is, the unimolecular transition states are "tighter", which is not surprising given the geometric constraints associated with the unimolecular reaction. All other things being equal, tighter transition states permit quantum mechanical tunneling to occur to a greater extent than for looser transition states, as quantified in more detail below.

Table S4 of the Supporting Information provides selected geometrical parameters for the tuck-in complexes of ligand systems **1**−**3**. In all cases the tuck-in complexes feature longer *r*MC and shorter *r*MΩ distances, as well as slightly larger Ω−M−Ω angles than the corresponding Me- or Np-alkylated parent systems. In their *r*MC and *r*MΩ distances, these complexes resemble their Cp* metallocene analogues,[4] though the change induced in ∠ΩMΩ by the tuck-in (which may be ≥10° in $(Cp^*)_2$) is much reduced due to the structural rigidity imposed by the bridging *ansa* methylene group.[16] *D* values decrease by roughly 0.1 Å, which is again unsurprising given the steric demands of the tuck-in complex.

Unimolecular Alkane Displacement. Table 2 contains 299 K enthalpies for stationary points on the two unimolecular metathesis pathways, relative to starting methyl and neopentyl complexes, for all combinations of ligand and metal, with Cp* data included for comparison.[4] For L = Me, the tuck-in complexes derived from **1**−**3** are about 10 kcal mol^{-1} less enthalpically stable than those formed from $(Cp^*)_2MMe$. However, this difference in product enthalpies is only partially included in the enthalpies of activation: differences between **1**−**3** and $(Cp^*)_2MMe$ for the latter quantity are only about 2−4 kcal mol^{-1}. These trends are amplified somewhat in the case of L = Np. The tuck-in complexes derived from **1**−**3** are now 10−20 kcal mol^{-1} less enthalpically stable than those formed from $(Cp^*)_2MNp$. Note that the tuck-in complex enthalpies are relative to educts, so the larger differences predicted for Np compared to Me simply reflect the greater steric clash between the Np ligand and the Cp* rings compared to the *ansa* ligands. Again, differences in tuck-in complex stabilities are only partially reflected in activation enthalpies; those computed for **1**−**3** are about 4−5 kcal mol^{-1} larger than those for $(Cp^*)_2MNp$.

As noted above, in the case of L = Me the enthalpies of activation for **1**−**3** are slightly higher than those for $(Cp^*)_2MMe$. However, the magnitudes of the imaginary frequencies in the *ansa*-ligated TS structures are slightly larger than those previously computed for $(Cp^*)_2MMe$.[4] Because quantum mechanical tunneling is more efficient when (1) barriers are lower and (2) barriers are tighter, the variations in barrier heights and imaginary frequencies have opposite effects on κ (cf. eqs 3 and 4), and indeed the two effects roughly cancel one another so that computed transmission coefficients are fairly insensitive to the nature of the aromatic ligand when L = Me (Table 2). This is *not* the case, however, for L = Np. In that case the substantially larger increase in the enthalpy of activation reduces the transmission coefficients computed for **1**−**3** relative to $(Cp^*)_2MNp$ by factors of 5 to 10 depending on the particular case.

Table 3. Relative Enthalpies (kcal mol^{-1}, 299 K) for Stationary Points on the Bimolecular Reaction Coordinates for *ansa* Ligands 1−4 and Quantum Mechanical Transmission Coefficients (unitless) for Their Rate-Determining Steps

ligand	metal	Me	bi‡	Me	κ_{299}
L = methyl					
$(Cp^*)_2$[a]	Sc	0.0	23.2	0.0	32
	Y	0.0	19.6	0.0	45
	Lu	0.0	20.9	0.0	44
1	Sc	0.0	19.6	0.0	46
	Y	0.0	18.9	0.0	46
	Lu	0.0	18.9	0.0	58
2	Sc	0.0	19.9	0.0	52
	Y	0.0	18.9	0.0	47
	Lu	0.0	18.5	0.0	62
3	Sc	0.0	20.4	0.0	57
	Y	0.0	19.6	0.0	49
	Lu	0.0	19.1	0.0	66
4	Sc	0.0	20.6	0.0	55
	Y	0.0	19.6	0.0	49
	Lu	0.0	19.4	0.0	64
ligand	metal	Np	bi‡	Me	κ_{299}
L = neopentyl					
$(Cp^*)_2$[a]	Sc	0.0	19.7	−15.8	32
	Y	0.0	17.0	−10.6	45
	Lu	0.0	18.1	−12.2	44
1	Sc	0.0	17.5	−7.9	60
	Y	0.0	18.1	−4.3	69
	Lu	0.0	18.0	−5.2	58
2	Sc	0.0	18.6	−8.2	36
	Y	0.0	18.0	−4.4	72
	Lu	0.0	18.2	−5.1	60
3	Sc	0.0	19.0	−7.5	42
	Y	0.0	18.7	−4.1	83
	Lu	0.0	18.6	−4.9	70
4	Sc	0.0	19.3	−7.6	47
	Y	0.0	19.0	−4.0	93
	Lu	0.0	18.9	−5.0	75

[a] Values taken from ref 4b.

Bimolecular Alkane Metathesis. Table 3 contains 299 K enthalpies of activation for all metal−ligand combinations, again with $(Cp^*)_2$ included for comparison.[4] For L = Me and M = Sc or Lu, activation enthalpies with the *ansa* ligands **1**−**4** are reduced by 2−4 kcal mol^{-1} compared to $(Cp^*)_2MMe$, consistent with the increased accessibility to the metal afforded by the narrow bite angle associated with the *ansa* ligand.[7,15,16] In the case of L = Me and M = Y, the larger ionic radius of Y mitigates this effect so that the activation enthalpies are insensitive to the nature of the ligand. In no case does methylation of the ligand have much influence on the activation enthalpies.

For L = Np, the exothermicity of metathesis is 6−8 kcal mol^{-1} larger for $(Cp^*)_2MNp$ compared to the *ansa* ligated systems **1**−**4**, again consistent with greater steric release in the free Cp*-ligated system. The influence of this greater exothermicity on the activation enthalpy acts to counterbalance the increased accessibility afforded by the *ansa* ligands so that in most instances the activation enthalpies for **1**−**4** are within 1 kcal mol^{-1} of those for $(Cp^*)_2MNp$. Again, there is little influence from ring methylation.

With respect to quantum mechanical tunneling, the similarities in activation enthalpies and imaginary frequencies between all of the various systems are such that κ ranges only from 32 to 93 for the bimolecular methathesis. This is in contrast to the

unimolecular reaction leading to a tuck-in complex, where tunneling for the *ansa* ligands is substantially reduced compared to $(Cp^*)_2ML$.

If we now consider the uni- and bimolecular reaction pathways in a reacting system, we see that the enthalpies of activation for the bimolecular reactions of **1**−**3** are in general about 15 kcal mol^{-1} more favorable than those for the analogous unimolecular reactions leading initially to tuck-in complexes (**4** has similar reactivity in the bimolecular case but cannot undergo unimolecular reaction since it lacks methyl groups on the indene five-membered ring). To compute rates from first principles, we must additionally consider the contribution of entropy to free energies of activation. There is some uncertainty in the computation of the absolute entropies for systems like those studied here, which are characterized by many low-frequency normal modes not well represented as harmonic oscillators[6] (a particular example of this inadequacy has been provided by Raynaud et al.,[30] who observed significant deviations between the harmonic-oscillator approximation and free energies of activation computed directly from Car−Parrinello dynamics for the reaction of H_2 with Cl_2LaH and Cl_2LaMe). Moreover, the gas-phase entropy of activation is not always an accurate predictor of the equivalent quantity in solution.[5q,31]

Nevertheless, with all of these caveats in mind we compute the 299 K entropy of activation for the bimolecular reaction to be about 27 eu higher than that for the unimolecular process. Such a difference corresponds to about 8 kcal mol^{-1} in free energy at 299 K. Thus, on the basis of a remaining difference in free energy of 7 kcal mol^{-1} ($H - TS$) and assuming a 1 M concentration of methane as a reactant, transition-state theory predicts that the rate of the bimolecular reaction will in every instance exceed the rate of the unimolecular reaction by about 5 orders of magnitude.[6] As transmission coefficients for the uni- and bimolecular reactions fail to differ by even 1 order of magnitude at this temperature, the unimolecular pathway is clearly of no consequence with the *ansa* ligands, and even significantly reduced concentrations of reactive methane would not be expected to change this situation. We note the contrast with the case of, say, $(Cp^*)_2ScNp$, where the difference in uni- and bimolecular activation *enthalpies* is only 7.5 kcal mol^{-1} and tunneling is about 1 order of magnitude more efficient for the unimolecular reaction at 299 K. In that case, even methane concentrations of 1 M would be expected to permit reaction via both pathways to be simultaneously operative.

In conclusion, compared to Cp* the *ansa* ligands examined here decrease the activation enthalpies for bimolecular reactions of group III methyl metallocenes with methane by 2−4 kcal mol^{-1}. The reactivities of corresponding neopentyl metallocenes, however, are largely unaffected because greater accessibility to metal centers with the *ansa* ligands is largely offset by relief of reactant strain associated with the sterically demanding neopentyl ligand. Activation enthalpies for unimolecular loss of methane or neopentane via the formation of a tuck-in complex are 4−6 kcal mol^{-1} larger with the *ansa* ligands studied here than with Cp*, so that this pathway cannot compete kinetically with bimolecular reaction. Quantum mechanical tunneling along the H atom transfer coordinates is predicted to accelerate all of the metathesis reactions studied here by about an order of magnitude at 299 K.

Significance. To the extent that we are interested in qualitative trends associated with *ansa* ligation compared to less constrained metallocenes, the theory employed in this work should be secure. With respect to *quantitative* accuracy, it is informative to consider some results from other studies. In particular, Barros et al.[5q] examined the bimolecular methane metathesis reaction of $(Cp^*)_2MMe$ with M = Sc, Y, and Lu (i.e., the exact unconstrained systems considered here) and predicted enthalpies of activation of 22.8, 19.5, and 21.3 kcal mol^{-1}, respectively, at the B3PW91 level of density functional theory with a basis set similar to that used here. These barriers are about 4 kcal mol^{-1} smaller than those that we compute with MPW1K,[4b] which difference is expected given the greater percentage of exact HF exchange in the MPW1K functional. As the MPW1K functional was specifically optimized for H atom exchange reactions,[25] there is good reason to expect that it will be more accurate for the metathesis reactions studied here.

This point may be evaluated in additional detail, as may the accuracy of the Skodje−Truhlar tunneling approach, by comparing the semiclassical enthalpies of activation computed from an Eyring plot of tunneling-corrected experimental rate constants to those computed directly from theory at the MPW1K level. Using the rate constants of Sadow and Tilley[2h] for the bimolecular reaction of $(Cp^*)_2ScNp$ with methane, the enthalpy of activation after correcting for tunneling is 20.5 kcal mol^{-1},[4b] which is in excellent agreement with the MPW1K value of 19.7 kcal mol^{-1} (Table 3). On the basis of this analysis, we expect the results reported here to have quantitative utility as well.

Acknowledgment. We thank Don Tilley for stimulating discussions. This work was supported by NSF grants CHE-0203446 and CHE-0610183.

Supporting Information Available: Cartesian coordinates and tables of selected geometrical data for all optimized theoretical structures. This material is available free of charge via the Internet at http://pubs.acs.org.

OM0606237

(30) Raynaud, C.; Daudey, J.-P.; Jolibois, F.; Maron, L. *J. Phys. Chem. A* **2006**, *110*, 101.

(31) (a) Cooper, J.; Ziegler, T. *Inorg. Chem.* **2002**, *41*, 6614. (b) Sakaki, S.; Tatsunori, T.; Michinori, S.; Sugimoto, M. *J. Am. Chem. Soc.* **2004**, *126*, 3332. (c) Leung, B. O.; Reidl, D. L.; Armstrong, D. A.; Rauk, A. *J. Phys. Chem. A* **2004**, *108*, 2720. (d) Rotzinger, F. P. *Chem. Rev.* **2005**, *105*, 2003.